PER3 rs772027021 SNP induce pigmentation phenotypes of dyschromatosis universalis hereditaria

Hongyu Chen
Guizhou Medical University
Pingping Yang
Guizhou Medical University
Dan Yang
The Affiliated Hospital of Guizhou Medical University
Dongsheng Wang
Sichuan Cancer Hospital and Institute
Mao Lu
The First Affiliated Hospital of Chendu Medical College
Yadong Li
Guizhou Medical University
Zhiqiang Zhong
Guizhou Medical University
Jing Zhang
The Affiliated Hospital of Guizhou Medical University
Zhen Zeng
Guizhou Medical University
Zhi Liu
The Affiliated Hospital of Guizhou Medical University
Xu Jia
Chengdu Medical College
Qinghe Xing
Fudan University
Ding'an Zhou (460318918@qq.com)
Guizhou Medical University https://orcid.org/0000-0002-6614-9321

Research Article

Keywords: Dyschromatosis Universalis Hereditaria (DUH), Hyperpigmentation phenotype , PER3 SNP, SASH1 mutation

Posted Date: June 1st, 2022

DOI: https://doi.org/10.21203/rs.3.rs-1668227/v1

Abstract

Dyschromatosis universalis hereditaria (DUH) is a pigmentary genodermatosis characterized by a mixture of hyperpigmented and hypopigmented macules distributed randomly over the body. Although *Sterile Alpha motifs- and SH3 domain-containing protein 1* (*SASH1*) and *ATP-binding cassette subfamily B, member 6*(*ABCB6*) have been identified as the causative genes for this disorder, there are still some cases with unknown pathogenic genes. In this study, whole exome sequencing, data analysis and sanger sequencing were utilized in a four-generations extended Chinese family with DUH. A single nucleotide polymorphism (SNP) (c. 517C > T (p.P173S, rs772027021) variant in the exon 5 of *Period Circadian Regulator 3* (*PER3*) (NM_001289861), was found in each affected individuals of the DUH family and the c. 517C > T SNP of *PER3*(*PER3* ^{rs772027021} SNP) and a novel c. 1574C > G (p.T525R) mutation in exon 14 of *SASH1* were both found in the proband. Increased melanin syntheses were induced by the *PER3* ^{rs772027021} SNP in melanocytes of the affected epithelial tissues. Mutated *SASH1* or *PER3* ^{rs772027021} *SNP* alone, or mutated *SASH1* and *PER3* ^{rs772027021} *SNP* synergistically caused more synthesized melanin, respectively *in vitro.* We also phenotypically characterized a commercially available zebrafish mutant line that harbored *PER3* ^{rs772027021} SNP to induce proliferative melanocytes *in vivo*. Our studies firstly revealed the *PER3* SNP may be as the pathogenic gene for a novel DUH subtype which was of delayed dominance and mutation of *SASH1* and *PER3* cooperatively promote hyperpigmentation phenotypes.

Introduction

Dyschromatosis universalis hereditaria [DUH; Online Mendelian Inheritance in Man (OMIM) 127500] is a rare autosomal dominant genodermatosis initially described by Ichikawa and Hiraga in two generations of two families in 1933(**Ichigawa T** 1933). This disorder is characterized by asymptomatic hyperpigmented and hypopigmented macules extensively distributing over the trunk, limbs, and sometimes the face(Al Hawsawi et al. 2002; Stuhrmann et al. 2008). In infancy or early childhood, lesions of irregular size and shape begin to appear(Al Hawsawi et al. 2002; Sethuraman et al. 2002; Urabe and Hori 1997). The lesions dominantly in the skin appear on the face, trunk and extremities in the affected individuals, but not involved in of palms and soles(Al Hawsawi et al. 2002) and abnormal lesions of hair and nails have also been reported(Sethuraman et al. 2002). We discovered three Chinese DUH pedigrees with dyschromatosis symmetrica hereditaria (DSH) in 2003(Xing QH 2003) with autosomal- dominant inheritance and diagnosed as DUH (Stuhrmann et al. 2008). Three additional variants in *SASH1* (E509K, L515P, and Y551D) associated with DUH in two Chinese families and one American family were identified by us to induce increased migration of melanoma cells(Zhou et al. 2013), mediates skin melanogenesis through a cascade of p53/α-MSH/ POMC/ Gαs/SASH1(Ding' An Zhou 2017), and crosstalk with ERK1/2-CREB cascade through MAP2K2 to promote melanogenesis(Zhou et al. 2017). Additionally, increasing evidences suggest that *SASH1* variants are associated with genodermatosis or DUH(Courcet et al. 2015; Hongzhou Cui 2020; Nan Wu 2020; Shellman et al. 2015). And recently, a p.T525R variant in *SASH1* has been reported in a sporadic patient with lentiginous phenotypes (Yuta Araki 2020).

Circadian rhythms are implicated in the mechanisms of refractive development. Two circadian clock gene clock and circadian rhythm–related genes *Per3* and *Cry1*, both expression of the two genes was influenced by altered visual input in chicks(Richard A. Stone 2020). PER3 is a member of the period family of genes and expressed in a circadian pattern in the suprachiasmatic nucleus, the primary circadian pacemaker in the mammalian brain. The downregulation of PER3 and other three circadian entrainment pathways relevant genes were involved in psoriasis(Zengyang Yu 2020).

In this study, *PER3* ^{rs772027021} SNP was found to be associated with pigmentation in an extended DUH family and *PER3* ^{rs772027021} SNP may be a novel casual gene to induce hyperpigmentation phenotypes. The hyperpigmented phenotypes did not appear until early 30s-years old in the affected individuals with *PER3* ^{rs772027021} SNP, which may indicate a novel DUH subtype may be caused by *PER3* ^{rs772027021} SNP. The *PER3* ^{rs772027021} SNP and the SASH1 c. 1574 C > G (p.T525R) variant synergistically induced the pigmentation phenotypes in the proband within the family.

Materials And Methods

Human subjects

All biological samples were obtained after written informed consent. The study was performed in accordance with the Declaration of Helsinki protocols and approved by the ethics committee of the respective institution.

Exome Sequencing and data analysis

1. DNA extract and exome sequencing Genomic DNA extracted from peripheral blood for each sample was fragmented to an average size of 180~280bp and subjected to DNA library creation using established Illumina paired-end protocols. The Agilent SureSelect Human All ExonV6 Kit (Agilent Technologies, Santa Clara, CA, USA) was used for exome capture according to the manufacturer's instructions. The Illumina Novaseq 6000 platform (Illumina Inc., San Diego, CA, USA) was utilized for genomic DNA sequencing in Novogene Bioinformatics Technology Co., Ltd (Beijing, China) to generate 150-bp paired-end reads with a minimum coverage of 10× for ~99% of the genome (mean coverage of 100×).

2. Data analysis After sequencing, basecall files conversion and demultiplexing were performed with bcl2fastq software (Illumina). The resulting fastq data were submitted to in-house quality control software for removing low quality reads, and then were aligned to the reference human genome (hs37d5) using the Burrows-Wheeler Aligner (bwa)(Li and Durbin 2009), and duplicate reads were marked using sambamba tools(A. Tarasov 2015).

3. SNP/INDEL calling Single nucleotide variants (SNVs) and indels were called with sam tools to generate gVCF(Li et al. 2009). The raw calls of SNVs and INDELs were further filtered with the following inclusion

thresholds: 1) read depth > 4; 2) Root-Mean- Square mapping quality of covering reads > 30; 3) the variant quality score > 20.

4. CNV calling The copy number variants (CNVs) were detected with software CoNIFER (V0.2.2)(Krumm et al. 2012).

5. Annotation Annotation was performed using ANNOVAR (2017June8)(Wang et al. 2010) . Annotations included minor allele frequencies from public control data sets as well as deleteriousness and conservation scores enabling further filtering and assessment of the likely pathogenicity of variants.

6. Rare variants filtering Filtering of rare variants was performed as follows: (1) variants with a MAF less than 0.01 in 1000 genomic data (1000g_all)(1000 Genomes Project Consortium 2015), esp6500siv2_all, gnomAD data (gnomAD_ALL and gnomAD_EAS) and in house Novo- Zhonghua exome database from Novogene; (2) Only SNVs occurring in exons or splice sites (splicing junction 10 bp) are further analyzed since we are interested in amino acid changes. (3) Then synonymous SNVs which are not relevant to the amino acid alternation predicted by dbscSNV are discarded; The small fragment non-frameshift (<10bp) indel in the repeat region defined by Repeat Masker are discarded. (4) Variations are screened according to scores of SIFT(Kumar P 2009), Polyphen(Adzhubei et al. 2010), MutationTaster(Schwarz et al. 2010) and CADD(Kircher et al. 2014) softwares. The potentially deleterious variations are reserved if the score of more than half of these four softwares support harmfulness of variations(Muona et al. 2015). Sites(>2bp) did not affect alternative splicing were removed.

7. ACMG classify In order to better predict the harmfulness of variation, the classification system of the American College of Medical Genetics and Genomics (ACMG) was used. The variations are classified into pathogenic, likely pathogenic, uncertain significance, likely benign and benign(Richards et al. 2015).

8. Genetic linkage analysis To identify the DUH loci, we performed independent genome-wide scan for linkage in the multi-generational family. This linkage analysis using merlin tools and the perl, combined with the family high throughput sequencing data and the HapMap database of Chinese population (CHB) allele frequency, using the known SNP as a marker linkage analysis, get the chain candidate area.

9. Pedigree analysis Given to the characteristics of the pedigree, heterozygous, homozygous and compound heterozygous variants were considered to be candidate causal variations.

10. Kinship analysis Relationship between proband and parents was estimated using the pairwise identity-by-descent (IBD) calculation in PLINK(Purcell et al. 2007). The IBD sharing between the proband and parents in all trios is between 45% and 55%.

Sanger sequencing

Primers used in the *PER3*, *SASH1, DPP10, KYNU*, *CELSR1, GLMN* and *SFTA3* variants validation and mutation analysis are listed in Supplemental Table S1. PCR products from genomic DNA were sequenced using an ABI3730XL DNA Analyzer (International Equipment Trading, Vernon Hills, IL). Sanger sequencing

was used to confirm the presence and identity of variants in the candidate gene identified via exome sequencing and to screen the candidate gene in the affected individuals and the unaffected individuals in the DUH family.

Immunohistochemistry

To examine the expression of SASH1、PER3, Ki67 and MART1 in skin, the normal foreskin samples from a 14-year-old- teenagers and the skin epithelial tissues of the hyperpigmented and hypopigmented lesional areas on the thigh and elbow of the proband and the shanks of the other affected individuals were stained with rabbit anti-PER3 antibody (ab224594, abcam, USA), rabbit anti-SASH1 polycolonnal antibody(pAb) (NBP-26650, Novus Biologicals, LLC,USA), rabbit anti-Ki67(27309-1-AP1) (Proteintech Group, Inc.,Wuhan,China) and rabbit anti-Melan A(MART1) antibody (bs-0051R) (Beijing Biosynthesis Biotechnology CO., LTD.). These skin epithelial tissues were fixed in 10% formalin at 4℃ for 24 h and then embedded in paraffin. Paraffin sections (5μm-thick) were incubated at 60℃ for 3 hr and then deparaffinized and rehydrated using xylene and an ethanol gradient. The immunohistochemical analyses procedure were mainly referred to our previous reports

Melanin staining

Melanin staining in the skin epithelial tissues of the normal controls and the affected individuals in the DUH family was performed as previously described(Zexi Xu 2020; Zhou et al. 2013).

Gene cloning、site- directed mutagenesis and virus packaging

The myc-DDK-tagged human period homolog 3(*PER3*) expression vector (RC217739, OriGene Technologies Inc. Ltd) was sequenced to identify the correctness of *PER3* sequence. The nucleotide 517"C" of *PER3* were mutated into "T" by site-directed mutagenesis using KOD-Plus- Mutagenesis kit (TOYOBO, Japan). The cDNA sequence of Human *PER3* (reference sequence of homo sapiens *PER3* : NM_001289861) were synthesized and 3×HA sequences were added after the initiation codon of *PER3* CDS sequence. The nucleotide 517"C" of *PER3* were mutated into "T" by site-directed mutagenesis technology. The wild type *PER3* and the $PER3^{C517T}$ SNP mutant were cloned into adeasy 014- pAdEasy- EF1- MCS- CMV-EGFP adenovirus vector. The cDNA sequence of *SASH1* (reference sequence of homo sapiens SASH1: NM_015278.5) were synthesized and 3×Flag sequences were added after the initiation codon of *SASH1* CDS sequence. The nucleotide 1574 "C" of *SASH1* were mutated into "G" by site-directed mutagenesis technology. The wild type SASH1 and the mutant type *SASH1* were cloned into adeasy014- pAdEasy- EF1- MCS- CMV-EGFP adenovirus vector via the restrict enzyme site of EcoRI and BamHI. The recombined adeasy014- pAdEasy- EF1-MCS-CMV-EGFP adenovirus were packaging by the and HanBio biological technology Co. ,Ltd, China.

Cell culture、transfection and infection

Human embryonic kidney 293T cells were obtained from the Cell Bank of Chinese Academy of Sciences(Shanghai, China). All cell lines were maintained in Dulbecco's Modified Eagle's Medium (HyClone Laboratories,Inc., Logan, UT, USA) supplemented with 10% BI fetal bovine serum (Bioind, Israel) and cultured at 37ºC with 5% CO2. The transfection procedure of GFP-SASH1 and myc-PER3 vectors were mainly referred to our previous reports(Ding' An Zhou 2017; Zhou et al. 2017). The infection of adenovirus was performed according to the procedure provided by the manufactures.

Immunoblotting

Most western blot were performed as previously described(Ding' An Zhou 2017; Zhou et al. 2017) .The primary antibodies used in western blot were as follows anti-GFP antibody (M20004M , Abmart Shanghai Co. ,Ltd., Shanghai, China)，anti-SASH1 antibody (NBP1-26650, Novus Biologicals, LLC) and anti-PER3 antibody (ab224594, Abcam, Cambridge, UK) .

Melanin quantification

At 48hr after transfection or infection，the B16 cells infected or transfected with the adeasy014- pAdEasy-EF1- MCS-CMV-EGFP- adenovirus overexpressing wild type and mutated PER3,SASH1 and HA-SFTA3 were washed with GenMed leaning liquid provided by the manufacturer (GenMed Scientifics Inc.), lysed with GenMed lysis buffer at 4°C for 30 min and proceeded with 16,000 0 g centrifugation for 5 min. at 4°C. The cell lysates of B16 were centrifuged at 16,000 0 g for 5 min at 4°C, and 10μl of supernatant was implemented to protein concentration determination. The supernatant was removed, 500μl of GENMED treating fluid was added to cell deposits and mixed and centrifuged at 16,000 g for 5 min. The supernatant was removed, and 500μl of GENMED dissolving solution was added into cell deposits and mixed. 500μl of GENMED buffer was added and stored at 60°C for 30 min avoiding exposure. The melanin content was determined by measuring the absorbance at 360 nm wavelength. SK-MEL-1 infected cells(10^6 cells per well) in 10-cm dishes were lysed with 1 M NaOH at 80℃ for 2 hr. After centrifugation at 12,000× g for 10 min at room temperature, the supernatants were transferred to fresh tubes and melanin content was determined in triplicate for each sample by measuring the absorbance at 405nm in a spectrophotometer and expressed as microgram of melanin per mg protein. Synthetic melanin (Sigma, St. Louis, MO, USA) was used to plot a standard curve to calculate the melanin content in SK-MEL-1 cells (Wen-Shyan Huang 2018).

Phenotype characterization of the *PER3*^{P173S} SNPand the *GLMN* c.561delT variant in zebrafish embryos.

Bioinformatics analysis of whether human *PER3* and zebrafish *per3* are orthologous genes. Whether human *PER3* and zebrafish *per3* are orthologous genes was analyzed using the online Ensembl database.

Using zebrafish embryos as a reactor to verify the function of the *PER3*^{P173S} SNPand the *GLMN* c.561delT variant of human. Wild type human *PER3* and *GLMN* cDNA were synthesized and cloned into pXT7 vector. According to the mutations of *PER3* c.C517T and the *GLMN* c.561delT , site-direct

mutagenesis was performed as per the protocol provided by KOD-Plus- Mutagenesis kit (TOYOBO, Japan) using the site-direct mutagenesis primers (Supplemental Table S11) of *PER3* and *GLMN*. Site directed mutation results of *PER3* and *GLMN* was verified by Sanger sequencing. Linearization of expression plasmid of wild type and mutant type *PER3* and *GLMN* was acquired by the SalI digestion. The linearization products was purified by the PCR clean up kit (Axygen). *In vitro* transcription was performed using mMESSAGE mMACHINE™ T7 Ultra Transcription Kit (Ambion). The mRNA transcribed *in vitro* was purified according to the protocol provided by the mMESSAGE mMACHINE™ T7 Ultra Transcription Kit (Ambion) by adding the lithium Chloride Precipitation Solution(Ambion) and 75% ethanol and resolved in RNase free H_2O. Agarose gel electrophoresis (1%) was used to identify the purified mRNA's integrity and the concentrations of purified mRNA was measured. The fertilized eggs of zebrafish were collected according to the conventional method. 20,100 and 250 ng/μl purified *PER3* mRNA and 25,100 and 250 ng/μl purified *GLMN* mRNA were micro-injected into zebrafish fertilized eggs. The survival rate of zebrafish fertilized eggs at 24 hpf was counted and the expression of *PER3* and *GLMN* in zebrafish fertilized eggs was detected with Qrt-PCR. 72 hpf was selected as a reference time point to characterize the pigmentation phenotype of zebrafish based on the previous reports (Sairah Yousaf 2020; Yongfei Yang 2018).

Statistical analysis

Data were analyzed using a homogeneity of variance test and one-way ANOVA was used for multiple comparisons using the least significant difference in SPSS16.0 to generate the required *P*-values. *P*-values of less than 0.05 were considered statistically significant. Data are presented as means±SDs. The cartograms were made and plotted using GraphPad Prism 5.

Results

Clinical features

We characterized a four-generation extended Chinese family with DUH in Zhaoyang, Hubei, China, in which the disease was transmitted in an autosomal dominant manner (Fig. 1A). The proband (III-6) was an early 30s woman who had normal skin at birth. The lesions occurred in a symmetrical pattern and were most obvious on the face, neck, trunk, and the dorsa of her hands and bottom. Hyperpigmented macules appeared initially on her face at the toddler age, and then the hyperpigmented macules became bigger and were evenly distributed freckles and the color of these macules deepened. Hypopigmented macules began to appear on the neck, elbows, knees, and phalangeal joints of the proband at the age of early adolescence. Her palms and soles, oral mucosa, hair, nails, and teeth were normal. After adulthood, irregularly shaped, asymptomatic hyper- and hypopigmented macules was presented over the face, neck, the abdomen and back, the dorsal aspects of the hands and the arms, the thighs, calves and hips (Fig. 1B and Supplementary Table S2).

The affected individuals including her grandmother（I-2）father（II-3）, fifth aunt(II-10), sixth uncle(II-11) and younger female cousin（III-12） of the proband all had sporadic or disseminated hyperpigmented and hypopigmented macules on her or his limbs(I-2,II-3, II-10 and III-12), his trunk shoulder back（II-3） and his facial regions and submaxill (II-11)(Fig. 1B-1E, and Supplementary Table S2). The pigmented lesions of II-3 affected individual were concentrated on the his trunk shoulder back and his hyperpigmented lesions were diffusely distributed (Fig. 1C) . The pigmented lesions of II-10 affected individual were concentrated in both lower limbs (Fig. 1D). The pigmented lesions of II-11 affected individual were focused in his ears (Fig. 1E). These five affected individuals all had hypopigmented or/and disseminated hyperpigmented macules, no skin atrophy, telangiectasia, inflammation, etc. These clinical symptoms supported the diagnosis of pigment abnormality in these five affected individuals. DUH is characterized by asymptomatic hyperpigmented and hypopigmented macules that occur in a generalized distribution over the trunk, limbs, and sometimes the face(Al Hawsawi et al. 2002; Sethuraman et al. 2002) . So, these five affected individuals were likely to be diagnosed with DUH.

According to their self memories and descriptions and the hyperpigmented and hypopigmented macules were intertwined and appear on their face, limbs and trunk of the DUH affected individuals(I-2, II-3, II-10 , II-11 and III-12) at the age of 30 (Fig. 1C-1F, and Supplementary Table S2) . However, the phenotypes of pigmentation abnormality of the proband were significantly obvious than those of the five DUH affected individuals (I-2, II-3, II-10, II-11 and III-12). The family's members' clinical characteristics are summarized in Supplementary Table S2.

The DUH pedigree was ascertained by two experienced dermatology doctors of the Affiliated Hospital of Guizhou Medical University and the First Affiliated Hospital of Chengdu Medical College and all of these patients were diagnosed as having the clinical phenotypes of DUH. DUH should be considered in the differential diagnosis of all cases manifesting with mixed hyper and hypopigmented macules and biopsy specimens should be obtained to confirm the diagnosis(Sasan Dogohar 2021). We further confirmed the phenotypes of increased melanin pigmentation in the affected skin epithelial tissues in the II-3 and II-10 affected individuals and the proband (III-6) of this family using melanin staining. Melanin staining assays revealed that excessive melanin pigmentation was detected both in the basal layers and the suprabasal layers of the proband's hyperpigmented macules(Fig. 2B). Less melanin and mosaic-like melanin distribution were observed in the hypopigmented macules of the proband (Fig. 2C). Like those of the proband, increased melanin pigmentation and mosaic-like melanin distribution were also presented in the basal layers and the suprabasal layers of hyperpigmented macules of the II-3 and II-10 affected individuals (Fig. 2D-2G).

Whole exome sequencing identifies the candidate genes in the family.

We subjected the exomes of five affected (I-2, II-3, II-10, III-6 and III-12) and five unaffected (I-1, II-1, II-4, II-13, and III-5) individuals to whole exome sequencing. Approximately 100million bases per individual were mapped and about 60 million bases were sequenced. Variants with a MAF less than 0.01 in databases including 1000 genomic data (1000g_all), and in house Novo-Zhonghua exome database are

identified, SNVs occurring in exons or splice sites were analyzed, synonymous SNVs were discarded, and variations were screened according to the scores of the pathogenicity prediction programs including SIFT(Kumar P 2009), Polyphen(Adzhubei et al. 2010), MutationTaster(Schwarz et al. 2010) and CADD software(Kircher et al. 2014). The variations were classified into pathogenic, likely pathogenic, uncertain significance, likely benign and benign according to the classification system of the American College of Medical Genetics and Genomics (ACMG)(Richards et al. 2015).

This linkage analysis in the multi-generational family were performed to get the chain candidate area using merlin tools and the perl combined with the family high throughput sequencing data and the HapMap database of Chinese population (CHB) allele frequency using the known SNP as a marker linkage analysis. A SNP for the disease-related pathogenic mutation was defined as one that exclusively existed in the five affected individuals with clinical phenotypes but did appear in the five unaffected individuals without clinical phenotypes of the family. **Twenty eight** variants remained and were located on multiple chromosomes. A c. 517C>T (p.P173S, rs772027021) variant in the exon 5 of *PER3*(NM_001289861) , a c.211delC(p.L71fs) variant in the exon 3 of surfactant associated 3 (*SFTA3*) (NM_001101341), a c. 716C>T (p.A239V, rs199529102) variant in the exon 9 of *kynureninase* (*KYNU*) (NM_ 001199241.2) and a c.561delT variant in *the* exon 5 of *Glomulin* (*GLMN*) (NM_053274.3) were screened to be the potential pathogenic mutations based on the pathogenicity prediction programs before most individuals in the DUH family whose blood was drew and their DNA were performed with Sanger sequencing afterwords. Their DNA of twenty four individual in the 31 ones-extended DUH family were performed with Sanger sequencing to identify the causative gene.

PER3^{rs772027021} SNP which was a missense SNV and abbreviated as *PER3*^{P173S} SNP subsequently was found in 6 affected individuals with hyper-pigmented and hypo-pigmented phenotypes whose DNA was analyzed with whole exome sequencing (Supplementary Table S2). The scoring of pathogenicity prediction programs supported that the locus of *PER3*^{P173S} SNP was predicated to be harmful (Supplementary Table S3). In order to analyze the *PER3*^{P173S} SNP in more individuals in the extended DUH family，twenty four individuals among the 31-people extended family agreed to draw their blood to identify the*PER3*^{P173S} SNP in their DNA. Sanger sequencing analyses showed that the *PER3*^{P173S} SNP occurred in seven affected members including the affected individuals of II-11 and III-9 who joined later, but not in any of the seventeen unaffected individuals of the family al (Fig. 3A and 3E, Supplementary **Table S2** and **Table S3**). The III-9 affected individuals with the *PER3*^{P173S} SNP whose age range was at 26-30 and had no hyperpigmented phenotypes according to his own examination. According to their own account of his father，uncle and aunt, the hyperpigmented macules began to appear at about 30-years old, which indicated that the hyperpigmented phenotypes induced by *PER3*^{P173S} SNP didn't appear until 30 years old. The locus rs2859387, rs228696, rs17031614, rs201662971 and rs199947375 of *PER3* were collectively found in five unaffected individuals (Supplementary Table S4). The locus rs228669, rs35733104, rs17031614 and rs2640908 of *PER3* were found in the III-5 unaffected individuals (Supplementary Table S4). The pathogenicity predication of *PER3*^{P173S} SNP was performed with the VarSome tool (https://varsome.com/). *PER3*^{P173S} SNP was also predicated to be damaging or

deleterious by six tools of CADD predication software, one tool of individual predication software and one tool of Meta score and pathogenicity score supported the SNP was harmful (Supplementary **Table S5**).

A c.211delC(p.L71fs) variant in the exon3 of *SFTA3* was found in six affected individuals(I-2, II-3, II-10, II-11, III-6 and III-12) with hyper-pigmented and hypo-pigmented phenotypes whose DNA was analyzed with whole exome sequencing. And the II-7 unaffected individual was identified to have c.211delC(p.L71fs) variant of *SFTA3* using Sanger sequencing afterwords (Supplementary **Table S6**). These results suggested that c.211delC(p.L71fs) variant of *SFTA3* did not cosegregate with the pigmented phenotypes in the DUH family.

A *KYNU* ^{rs199529102} SNP was detected in the affected individuals(I-2, II-3, II-10, III-6 and III-12), however was also found in the unaffected one(II-13), which indicate that *KYNU* ^{rs199529102} SNP did not co-segregate with the pigmented phenotypes (Supplementary **Table S7**). A rs1109866 SNP(c.G117A, p.L39L) in exon 1 of *ABCB6* which cause synonymous SNV was detected in five affected individuals(I-2, II-3, II-10, III-6 and III-12) and the *ABCB6* ^{rs1109866} SNP was predicted to be harmless as assessed by the pathogenicity prediction programs. An *ABCB6* ^{rs1109867} SNP was also found in the five affected individuals, however, assessment of the pathogenicity prediction programs did not support that this variant was predicated to be harmful (Supplementary **Table S8**).

According to our previous reports about DUH, a *SASH1* variant (rs770362998) were also included for consideration(Supplementary **Table S9**). However, the sanger sequencing revealed no mutation was detected on *SASH1* (data not shown). The genetic disease testing report provided by Chigene Translational Medical Research Center Co. Ltd. (Beijing, China) about the exome sequencing results of the proband showed that a c. 1574C>G(p.T525R) in the exon 14 of *SASH1* (NM_015278) was detected for prenatal diagnosis . Sangersequencing analysis was further performed to identify the C1574G *SASH1* mutation in the five affected (I-2, II-3, II-10, III-6 and III-12) and five unaffected (I-1, II-1, II-4, II-13, and III-5) individuals. Sangersequencing analysis demonstrated that c. 1574C>G (p.T525R) in the exon 14 of *SASH1* was only detected in the proband and not in other five affected or unaffected individuals (Fig. 3C). The c.C1574G *SASH1* variant was also detected the proband's aborted fetus (data not shown). A *SASH1* ^{rs208696} SNP was detected in three unaffected individuals (I-1, II-1 and II-4)and four affected ones(II-3, II-10, III-6 and III-12), which suggested that the *SASH1* ^{rs208696} SNP did not co-segregate with the pigmented phenotypes (Supplementary **Table S9**).

A c.561delT variant in *the* exon 5 of *GLMN* was found in the in the affected individuals (I-2, II-3, II-10, II-11 and III-12) and was also detected in the unaffected one(III-14). However, the c.561delT variant of *GLMN* was not detected in the proband. All of these indicated that the c.561delT variant of *GLMN* did not co-segregate with the pigmented phenotypes (Supplementary **Table S10**).

In the Twenty-four variants which were screened to be the potential pathogenic mutations based on the pathogenicity prediction programs except for *PER3*, *KYNU*, *SASH1* and *SFTA3*, detailed annotation results of the remaining 24 variants or SNP including *MYOC* ^{rs74315337} SNP, *CELSR1* ^{rs374501629} SNP, *ST3GAL5*

rs549326241 SNP, *DPP10* rs138159056 SNP, *DES* c.740delT variant, *UMPS* rs12191789 SNP, *BCHE* rs537434945 SNP, *EVC2* rs200140401 SNP, *ADAMTS6* rs147540204 SNP, *MAK* c.A1598G variant, *PKHD1* 6:51768842-T-A variant, *PHIP* rs200515013 SNP, *RAD54B* rs114216685 SNP, *HPS6* c.1687dupC variant, *ST14* c.C1819T variant, *TRPC4* rs757614572 SNP, *SF3B2* rs201160612 SNP, *LRRK2* rs34594498 SNP, *GCH1* rs770547722 SNP, *DUOX2* rs180671269 SNP, *DUOX2* c.G943T variant, *CRTC3* c.G967A variant, *AP2B1* 17:34036332-G-A variant and *GSS* rs113191242 SNP were indicated in Supplementary **Table S11**. The remaining 24 variants or SNP did not co-segregate with the pigmented phenotypes in the affected and unaffected individuals who were subjected to whole exome sequencing (Supplementary Table S11). The the Pro173 of PER3 and Thr525 site of SASH1 showed high conservation among different species (Fig. 3B and 3D) .

PER3 shows differential expression between the hyperpigmented and the hypopigmented macules.

We further investigated the expression of PER3 of the hyperpigmented macules and the hypopigmented ones in the II-3 and II-10 affected individuals and the proband. Immunohistochemical analysis revealed mosaic-like distribution and high expression of PER3 in the affected epidermis of hyperpigmented macules compared to those in the hypopigmented macules in the proband (Supplementary Fig. S1A). High expression of PER3 was detected in the affected epidermis of hyperpigmented macules compared to those in the hypopigmented macules in the II-3 and II-10 affected individuals (Supplementary Fig. S1B,1C). Th expression and distribution of SASH1 was also investigated. mosaic-like distribution and high expression of SASH1 in the affected epidermis of hyperpigmented macules compared to those in the hypopigmented macules in the proband (Supplementary Fig. S2A -2B). However, no differential expression of SASH1 was observed in the affected epithelial layers between the hyperpigmented macules and the hypopigmented ones of the II-3 and II-10 affected individuals (Supplementary Fig. S2C-S2F).

PER3 ^{P173S} **SNP and/or SASH1 mutation induce increased numbers of melanocytes in affected skin.**

To investigate the effects of ***PER3*** ^{P173S} **SNP** and/or *SASH1* ^{T525R} variant on the melanocyte proliferation, sections were stained with the proliferation marker, Ki67, and the melanocyte marker MART1 to identify the proliferation numbers of melanocyte in the affected epidermis. Compared to the epidermis of hypopigmented macules in the proband (III-6) with ***PER3*** ^{P173S} **SNP** and *SASH1* ^{T525R} variant, about 2 fold more proliferating cells (Ki67-positive cells) were showed in the epidermis of hyperpigmented macules (Fig. 4A, 4D). Compared to the epidermis of hypopigmented macules in the II-3 affected individual with *PER3* SNP，IHC analysis of Ki67 showed about 10 fold more proliferating cells in the affected epithelial tissues in the hyperpigmented macules of the II-3 affected individual (Fig. 4B , 4D). Compared to the epidermis of hypopigmented macules in the II-10 affected individual, about 25 fold more proliferating cells were demonstrated in the affected epithelial tissues in the hyperpigmented macules of the II-10 affected individual (Fig. 4C, 4D). Compared to the epidermis of hypopigmented macules in the proband (III-6), about 5 fold more melanocyte (MART1-positive cells) were showed in the epidermis of hyperpigmented macules (Fig. E, 4H). Compared to the epidermis of hypopigmented macules in the II-3 affected individual，IHC analysis of MART1 showed about 15 fold more melanocytes in the affected epithelial tissues in the hyperpigmented macules of the II-3 affected individual (Fig. 4F, 4H). Compared to

the epidermis of hypopigmented macules in the II-10 affected individual, about 10 fold more melanocytes were showed in the affected epithelial tissues in the hyperpigmented macules of the II-10 affected individual (Fig. 4G, 4H).

Increased melanin was induced by *PER3*^{P173S} SNP and/or *SASH1*^{T525R} variant.

We also assessed the effects of *PER3*^{P173S} SNP and/or *SASH1*^{T525R} variant on melanogenesis *in vitro*. Western blot indicated that mutant type SASH1 was upregulated in B16 cells (Fig. 5A,5B) and SK-MEL-1 cells (Fig. 5D ,5E). Melanin quantification suggested that increased synthesized melanin was induced by *PER3*^{P173S} SNP in B16 cells (Fig. 5C) and SK-MEL-1 cells (Fig. 5F) compared to that by wild type *PER3*, respectively. More synthesized melanin was induced by the cooperation between *PER3*^{P173S} SNP and *SASH1*^{T525R} variant compared to *SASH1*^{T525R} variant (Fig. 5C) in B16 cells. Enhanced synthesized melanin was induced by the cooperation between *PER3*^{P173S} SNP and *SASH1*^{T525R} variant compared to *SASH1*^{T525R} variant compared to *SASH1*^{T525R} variant and *PER3*^{P173S} SNP in SK-MEL-1 cells, respectively (Fig. 5F). More synthesized melanin was induced by overexpressed *SASH1*^{T525R} variant compared to wild type *SASH1* in B16 cells (Fig. 5C) and SK-MEL-1 cells(Fig. 6F). The *KYNU* c.C716T variant exhibited similar family distribution with that of *PER3*^{P173S} SNP (Supplementary Fig. S3A), however melanin quantification detection of B16 cells infected with *KYNU* ADV revealed that no increased melanin was induced by KYNU mutation (Supplementary Fig. S3B).

The *SFTA3* c.211delC variant also exhibited similar family distribution with that of *PER3*^{P173S} SNP (Supplementary Table S5). however, no increased melanin synthesis was caused by the introduction of wild type or mutant type of *SFTA3*(Supplementary Fig. S4A, S4B) . Enhanced melanin synthesis was not induced by the combination of WT-*PER3*+WT-*SFTA3* compared to that by wild type *PER3*. Also melanin was not increased by the combination of MT-*PER3*+MT-*SFTA3* compared to that by mutant type PER3(Supplementary Fig. S4E).

***PER3*^{P173S} SNP is essential for melanocyte proliferation and development *in vivo*.**

In this study,*PER3*^{P173S} SNP is firstly reported to induce the pigmented phenotypes in DUH affected individuals. The zebrafish is an ideal model for studying melanocyte differentiation(Webster et al. 2001; Yongfei Yang 2018). Homology of gene sequence of PER3 analyses from Ensembl database suggested that human *PER3* and zebrafish *per3* were homologous gene and there are collinear genes vamp3 (vamp3), UTS2 (uts2b), etc, which indicated human *PER3* and zebrafish *per3 are* orthologous genes (Fig. 6A). Homology analyses of amino acid sequence of PER3 suggested 37.1% homology of amino acid sequence was found between human and zebrafish (Supplementary Fig. S5).

In order to investigate the *in vivo* pathogenic effects of the variant in zebrafish, wild type and mutant type of *PER3* were transcribed into RNA *in vitro* and injected into zebrafish fertilized eggs. Quantitative RT-PCR detection of the *PER3* variant and wild type *PER3* genes in 24 hr post fertilization (hpf) fertilized eggs showed that the expression levels of all concentration injection groups were significantly increased,

which indicated that wild type *PER3* and *PER3*^{P173S} SNP were expressed in zebrafish(Fig. 6B) . 100 ng/μl was selected as the optimum dose for further studies based on the observed expression of *PER*3. We selected 72 hpf as a reference time point to characterize the pigmentation phenotype of zebrafish based on the previous reports (Sairah Yousaf 2020; Yongfei Yang 2018). As anticipated, a significantly considerable number of proliferative melanocytes were induced by *PER3*^{P173S} SNP compared to those of control group and wild type group (Fig. 6C and 6D). These results indicate that *PER3*^{P173S} SNP plays an important role in melanocyte proliferation and development in zebrafish *in vivo*. Additionally, no enhanced melanin synthesis was induced by the *GLMNc.561delT variant* compared to wild type GLMN in B16 cells (Supplementary Fig. S7A). no increased number of proliferative melanocytes were induced by the *c.561delT variant of GLMN* compared to those of control group and wild type group (Supplementary Fig. S7B, S7C) *in vivo*.

Discussion

DUH is pigmented dermatosis with genetic heterogeneity. Previous study reported three loci and two causal genes responsible for DUH : 2q33.3- q36.1 (*ABCB6*)(Cui et al. 2013; Liu H 2014; Lu et al. 2014; Nan Wu 2020; Zhang et al. 2013), 6q24.2-q25.2(*SASH1*)(Courcet et al. 2015; Ding' An Zhou 2017; Hongzhou Cui 2020; Nan Wu 2020; Xing QH 2003; Zhong et al. 2018; Zhou et al. 2017; Zhou et al. 2013) and 12q21-q23(Stuhrmann et al. 2008). In this study, we performed an integrated approach and found a *PER3*^{P173S} SNP or/ and a *SASH1*^{T525R} mutation in a DUH pedigree. Our study identifies a disease-causing SNP in *PER3* that is responsible for DUH. Our study may prove the novel pathogenic variant of *PER3* in the DUH pathogenesis and enrich the diagnosis of causal gene of DUH. Different from the DUH clinical phenotypes previously reported that these lesions of irregular size and shape always appear in infancy or early childhood (Cao et al. 2021; Hawsawi K 2012; Nan Wu 2020; Stuhrmann M 2008; Urabe and Hori 1997), in the study, the clinical symptoms did not appear until about 30 years old in the affected individuals, which may indicate a novel delayed dominant DUH subtype may be caused by the *PER3*^{P173S} SNP.

PER3 is an originally described as a core component of the circadian clock and one of the most robustly rhythmic genes in humans and animals. *PER3* variants, especially the human variable number tandem repeat (VNTR), are associated with diurnal preference, mental disorders, non-visual responses to light, brain and cognitive responses to sleep loss/circadian misalignment(Ding' An Zhou 2017). The onset age of a 99 affected homogeneous patients with bipolar disorder type I was influenced by the variable-number tandem-repeat (VNTR) polymorphism of *PER3* (Francesco Benedetti 2008). The diurnal preference was associated with *PER3* VNTR and the diurnal preference in young people is more closely associated with the *PER3* polymorphism(Kay H. S. Jones 2007). These observations indicate that the *PER3* polymorphism has associations with the onset age of mental illness. In this study, our observations indicated *PER3*^{P173S} SNP had associations with the onset age of the delayed dominant DUH in five affected individuals.

Two rare variants (P415A and H417R) occur at residues of *PER3* cause familial advanced sleep phase(FASP) and are associated with elevated Beck Depression(Luoying Zhanga 2016). Homozygosity for the longer allele (PER3(5/5)) had a considerable effect on sleep structure and the cognitive performance in response to sleep loss decreased significantly in the *PER3*(5/5) individuals, which revealed that this polymorphism in *PER3* predicts individual differences in the sleep-loss-induced decrement in performance(Antoine U Viola 2007). The *PER3*^{P173S} SNP causes a missense variant in the coding sequence of *PER3* and has not been reported to be of clinical significance (https://www.ncbi.nlm.nih.gov /snp/ rs772027021). In the study, *PER3*^{P173S} SNP is firstly reported to associate with skin hyperpigmentation, melanogenesis and melanocyte proliferation. In order to identify the functions of *PER3*^{P173S} SNP in the increased melanin pigmentation, melanoma cells and melanocytes were infected with wild type *PER3* and mutant-type *PER3*, and melanin quantification indicated that increased melanin synthesis was induced by *PER3*^{P173S} SNP compared to wild type PER3 and the negative control adenovirus(Fig. 5C and 5F). More importantly, *in vivo* functional analyses of human *PER3* in zebrafish verified that increased number of melanocytes was induced by *PER3*^{P173S} SNP (Fig. 6), which may interpret that pigmented phenotypes could be caused by *PER3*^{P173S} SNP in the DUH affected individuals. The sleep quality of the proband and the other patients in the DUH family was enquire about. These patients told they were of good sleep quality although they were of *PER3* ^{rs772027021} SNP.

SASH1 is a signaling adaptor protein of 1,247 amino acids containing an evolutionarily conserved SLY domain (401-555), an SH3 domain (557-614) and two SAM domains (633-697,1177-1241, annotation from the UniProt database)(Zexi Xu 2020). Increasing numbers of *SASH1* variants have been found to be associated with DUH(Courcet et al. 2015; Ding' An Zhou 2017; Hongzhou Cui 2020; Nan Wu 2020; Yuta Araki 2020; Zhou et al. 2017; Zhou et al. 2013). Apart from 3 additional variants in *SASH1* that were reported by us, which are located in the SLY domain of SASH1 (p.E509K, p.L515P, and p.Y551D)(Ding' An Zhou 2017; Zhou et al. 2017; Zhou et al. 2013), two identified SASH1 variants (p.Y551H(Zhong et al. 2018) and p.Q518P (Nan Wu 2020)) were associated with DUH, and are located in the highly conserved SLY domain. All these findings suggest that the SLY domain is functionally critical for skin pigmentation regulation and may represent a potential mutational hotspot region during the development of disease phenotype of DUH. The p.T525R variant in *SASH1* which was reported in a sporadic DUH Japanese patient, which causes lentiginous(Yuta Araki 2020). In this study, the p.T525R variant in *SASH1* cause hyperpigmentation phenotypes of DUH. *SASH1* p.T525R mutation was only detected in the proband and not in other affected and unaffected individuals in this DUH family, which indicated that the p.T525R variant in *SASH1* was a de novo mutation. *In vitro* assays revealed that increased synthesized melanin were induced by T525R *SASH1* mutant. Our findings may enrich the functions of *SASH1* variant in hereditary pigmentary diseases including DUH and lentiginous. In order to reveal the reasons that the clinical phenotypes of the proband are more serious than those of other patients in the DUH family, we analyze the relationship of *PER3*^{P173S} SNP and *SASH1*^{T525R} variant. Functional analyses in melanoma cells indicated that enhanced melanin synthesis was induced by the cooperation of *PER3*^{P173S} SNP and *SASH1*^{T525R} variant compared to that by *PER3*^{P173S} SNP and *SASH1*^{T525R} variant alone, respectively

(Fig. 5C,5F). Taken above, these results explain the underlying reasons that pigmentation phenotypes in the proband was more serious than those of other affected individuals.

In the twenty eight variants which were screened to be the potential pathogenic mutations based on the pathogenicity prediction programs, *SFTA3, KYNU* and *GLMN* exhibited high possibility to cause the hyperpigmentation phenotypes in the DUH family(Supplementary Table S5, Table S6 and Table S9). The variants of *SFTA3, KYNU* and *GLMN* demonstrated similar family distribution with that of *PER3*^{P173S} SNP and the *in vitro* and *in vivo* functions of these variants were investigated. Melanin quantification analyses indicated the *SFTA3* c.211delC variant alone or the combination of *SFTA3* c.211delC variant and *PER3*^{P173S} SNP had no effects on melanin synthesis compared to control or wild type *SFTA3* or mutant type *PER3* (Supplementary Fig. S4). No increased melanin synthesis was induced by the *KYNU* variant (Supplementary Fig. S3B). No increased melanogenesis was induced by the *GLMN* c.561delT variant *in vitro* and no increased number of proliferative melanocytes were induced *in vivo* (Supplementary Fig.S7).

Declarations

Acknowledgements We thank the Clinical Research Center at Affiliated Hospital of Guizhou Medical University for housing experiments. We thank Dehou Yu at Department of Dermatovenereology, the Affiliated Hospital of Guizhou Medical University for the disease diagnosis in the DUH family. We thank Nan jing YSY Biotech,Ltd. in Jiang shu, China for zebrafish husbandry and lines and injection of PER3 mRNA into zebrafish fertilized eggs and other functional assays.

Author contributions Ding'an Zhou made substantial contribution to the conception and design of the work; Qinghe Xing and Dongsheng Wang provided some constructive comments to analyze the results of the exome sequencing and sanger sequencing. Hongyu Chen, Pingping Yang, Dan Yang did most of the experiments, analyzed and interpreted the data; Yadong Li, Jing Zhang, Zhen Zeng and Zhiqiang Zhong participated in some experiments; Zhi Liu, Mao Lu participated the diagnosis of the pedigree Ding'an Zhou and Xu Jia drafted and revised the manuscript; All authors read and approved the final manuscript.

Funding This work was supported partly by the funds National Natural Science Foundation Project (31860319 and 32060165 to Ding'an Zhou) Guizhou Provincial Science and Technology Department Project (grant no: qian ke he zhicheng [2020]4Y125 and qian ke he jichu-ZK[2021] zhongdian 031 to Ding'an Zhou) ,and National Natural Science Foundation Project (31371274 to Qinghe Xing).

Compliance with ethical standards

Conflicts of interest The authors declare that they have no conflict of interest.

Ethics approval All procedures performed in studies involving human participants were approved by the ethics committee of the Affiliated Hospital of Guizhou Medical University and acquired the ethical approval documents (No.2020073K). The study was in accordance with the 1964 Helsinki declaration. Informed consent to participate in the study has been obtained from participants.

Informed consent to participate Written informed consent was obtained from all participants.

Informed consent for publication Consent for publication was obtained from all participants.

References

1. 1000 Genomes Project Consortium AA, Brooks LD, Durbin RM, Garrison EP, Kang HM, et al. (2015) A global reference for human genetic variation. . Nature 526: 68–74.
2. A. Tarasov AJV, E. Cuppen, I. J. Nijman, and P. Prins. (2015) Sambamba: fast processing of NGS alignment formats. Bioinformatics 31: 2032–2034.
3. Adzhubei IA, Schmidt S, Peshkin L, Ramensky VE, Gerasimova A, Bork P, Kondrashov AS, Sunyaev SR (2010) A method and server for predicting damaging missense mutations. Nat Methods 7: 248-9. doi: 10.1038/nmeth0410-248
4. Al Hawsawi K, Al Aboud K, Ramesh V, Al Aboud D (2002) Dyschromatosis universalis hereditaria: report of a case and review of the literature. Pediatr Dermatol 19: 523-6. doi: 10.1046/j.1525-1470.2002.00225.x
5. Antoine U Viola SNA, Lynette M James, John A Groeger, June C Y Lo, Debra J Skene, Malcolm von Schantz, Derk-Jan Dijk (2007) PER3 polymorphism predicts sleep structure and waking performance. Curr Biol 17: 613-618.
6. Cao L, Zhang R, Yong L, Chen S, Zhang H, Chen W, Xu Q, Ge H, Mao Y, Zhen Q, Yu Y, Hu X, Sun L (2021) Novel missense mutation of SASH1 in a Chinese family with dyschromatosis universalis hereditaria. BMC Med Genomics 14: 168. doi: 10.1186/s12920-021-01014-w
7. Courcet JB, Elalaoui SC, Duplomb L, Tajir M, Riviere JB, Thevenon J, Gigot N, Marle N, Aral B, Duffourd Y, Sarasin A, Naim V, Courcet-Degrolard E, Aubriot-Lorton MH, Martin L, Abrid JE, Thauvin C, Sefiani A, Vabres P, Faivre L (2015) Autosomal-recessive SASH1 variants associated with a new genodermatosis with pigmentation defects, palmoplantar keratoderma and skin carcinoma. Eur J Hum Genet 23: 957-62.
8. Cui YX, Xia XY, Zhou Y, Gao L, Shang XJ, Ni T, Wang WP, Fan XB, Yin HL, Jiang SJ, Yao B, Hu YA, Wang G, Li XJ (2013) Novel mutations of ABCB6 associated with autosomal dominant dyschromatosis universalis hereditaria. PLoS One 8: e79808. doi: 10.1371/journal.pone.0079808
9. Ding' An Zhou ZW, Zhongshu Kuang,Huangchao Luo, Jiangshu Ma□Xing Zeng□Ke Wang□Beizhong Liu□Fang Gong□Jing Wang□Shanchuan Lei□Dongsheng Wang□Jiawei Zeng□Teng Wang□Yong He□ Yongqiang Yuan□Hongying Dai□Lin He□Qinghe Xing (2017) A novel P53/POMC/Gαs/SASH1 autoregulatory feedback loop activates mutated SASH1 to cause pathologic hyperpigmentation. Journal of Cellular and Molecular Medicine 21: 802-815.
10. Francesco Benedetti SD, Cristina Colombo, Adele Pirovano, Elena Marino, Enrico Smeraldi (2008) A length polymorphism in the circadian clock gene Per3 influences age at onset of bipolar disorder. Neurosci Lett 445: 184-187.

11. Hawsawi K AK, Ramesh V et al. (2012) Dyschromatosis universalis hereditaria: report of a case and review of the literature. Pediatr Dermatol 19: 523–526.
12. Hongzhou Cui SG, Hongxia He, Huina Guo, Yuliang Zhang, Binquan Wang (2020) SASH1 promotes melanin synthesis and migration via suppression of TGF-β1 secretion in melanocytes resulting in pathologic hyperpigmentation. International Journal of Biological Sciences 16: 1264-1273.
13. **Ichigawa T** H (1933) A previously undescribed anomaly of pigmentation dyschromatosis universalis hereditaria. Jpn J Dermatol Urol 34: 360-364.
14. Kay H. S. Jones JE, Malcolm Von Schantz, Debra J. Skene, Derk-Jan Dijk, Simon N. Archer (2007) Age-related change in the association between a polymorphism in the PER3 gene and preferred timing of sleep and waking activities. J Sleep Res. 16: 12-16.
15. Kircher M, Witten DM, Jain P, O'Roak BJ, Cooper GM, Shendure J (2014) A general framework for estimating the relative pathogenicity of human genetic variants. Nat Genet 46: 310-5. doi: 10.1038/ng.2892
16. Krumm N, Sudmant PH, Ko A, O'Roak BJ, Malig M, Coe BP, Project NES, Quinlan AR, Nickerson DA, Eichler EE (2012) Copy number variation detection and genotyping from exome sequence data. Genome Res 22: 1525-32. doi: 10.1101/gr.138115.112
17. Kumar P HS, Ng PC. (2009) Predicting the effects of coding non-synonymous variants on protein function using the SIFT algorithm. Nat Protoc 4: 1073–1081.
18. Li H, Durbin R (2009) Fast and accurate short read alignment with Burrows-Wheeler transform. Bioinformatics 25: 1754-60. doi: 10.1093/bioinformatics/btp324
19. Li H, Handsaker B, Wysoker A, Fennell T, Ruan J, Homer N, Marth G, Abecasis G, Durbin R, Genome Project Data Processing S (2009) The Sequence Alignment/Map format and SAMtools. Bioinformatics 25: 2078-9. doi: 10.1093/bioinformatics/btp352
20. Liu H LY, Hung KK, Wang N, Wang C, Chen X, Sheng D, Fu X, See K, Foo JN, Low H, Liany H, Irwan ID, Liu J, Yang B, Chen M, Yu Y, Yu G, Niu G, You J, Zhou Y, Ma S, Wang T, Yan X, Goh BK, Common JE, Lane BE, Sun Y, Zhou G, Lu X, Wang Z, Tian H, Cao Y, Chen S, Liu Q, Liu J, Zhang F (2014) Genome-wide linkage, exome sequencing and functional analyses identify ABCB6 as the pathogenic gene of dyschromatosis universalis hereditaria. PLOS ONE 3: e87250.
21. Lu C, Liu J, Liu F, Liu Y, Ma D, Zhang X (2014) Novel missense mutations of ABCB6 in two chinese families with dyschromatosis universalis hereditaria. J Dermatol Sci 76: 255-8. doi: 10.1016/j.jdermsci.2014.08.015
22. Luoying Zhanga AH, 1, Pei-Ken Hsua, Christopher R. Jonesb, Noriaki Sakaic, Masashi Okuroc,Thomas McMahona, Maya Yamazakia, Ying Xua, Noriko Saigoha, Kazumasa Saigoha, Shu-Ting Lina, Krista Kaasika,Seiji Nishinoc, Louis J. Ptácek ˇ a and Ying-Hui Fu (2016) A PERIOD3 variant causes a circadian phenotype and is associated with a seasonal mood trait. Proc. Natl. Acad. Sci. U.S.A. 113: E1536-E1544.
23. Muona M, Berkovic SF, Dibbens LM, Oliver KL, Maljevic S, Bayly MA, Joensuu T, Canafoglia L, Franceschetti S, Michelucci R, Markkinen S, Heron SE, Hildebrand MS, Andermann E, Andermann F,

Gambardella A, Tinuper P, Licchetta L, Scheffer IE, Criscuolo C, Filla A, Ferlazzo E, Ahmad J, Ahmad A, Baykan B, Said E, Topcu M, Riguzzi P, King MD, Ozkara C, Andrade DM, Engelsen BA, Crespel A, Lindenau M, Lohmann E, Saletti V, Massano J, Privitera M, Espay AJ, Kauffmann B, Duchowny M, Moller RS, Straussberg R, Afawi Z, Ben-Zeev B, Samocha KE, Daly MJ, Petrou S, Lerche H, Palotie A, Lehesjoki AE (2015) A recurrent de novo mutation in KCNC1 causes progressive myoclonus epilepsy. Nat Genet 47: 39-46. doi: 10.1038/ng.3144

24. Nan Wu LT, Xiuxiu Li , Yuwei Dai , Xiaodong Zheng , Min Gao , Peiguang Wang. (2020) Identification of a Novel Mutation in SASH1 Gene in a Chinese Family With Dyschromatosis Universalis Hereditaria and Genotype-Phenotype Correlation Analysis. Front Genet 11: 841.
25. Purcell S, Neale B, Todd-Brown K, Thomas L, Ferreira MA, Bender D, Maller J, Sklar P, de Bakker PI, Daly MJ, Sham PC (2007) PLINK: a tool set for whole-genome association and population-based linkage analyses. Am J Hum Genet 81: 559-75. doi: 10.1086/519795
26. Richard A. Stone WW, Shanta Sarfare, Brendan McGeehan,K. Cameron Engelhart, Tejvir S. Khurana,3 Maureen G. Maguire, P. Michael Iuvone, and Debora L. Nickla (2020) Visual Image Quality Impacts Circadian Rhythm-Related Gene Expression in Retina and in Choroid: A Potential Mechanism for Ametropias. Invest Ophthalmol Vis Sci 61: 13.
27. Richards S, Aziz N, Bale S, Bick D, Das S, Gastier-Foster J, Grody WW, Hegde M, Lyon E, Spector E, Voelkerding K, Rehm HL, Committee ALQA (2015) Standards and guidelines for the interpretation of sequence variants: a joint consensus recommendation of the American College of Medical Genetics and Genomics and the Association for Molecular Pathology. Genet Med 17: 405-24. doi: 10.1038/gim.2015.30
28. Sairah Yousaf SS, , Muhammad A. Chaudhary, Rehan S. Shaikh, Saima Riazuddin, Zubair M. Ahmed (2020) Molecular characterization of SLC24A5 variants and evaluation of Nitisinone treatment efficacy in a zebrafish model of OCA6. Pigment Cell Melanoma Res. 33: 556–565.
29. Sasan Dogohar PA, Hamidreza Ghasemi Basir , Mohammad Jamshidi , Farshid Etaee (2021) Sporadic Dyschromatosis Universalis Hereditaria: A Second Case Report From Iran. Cureus 13: e16511.
30. Schwarz JM, Rodelsperger C, Schuelke M, Seelow D (2010) MutationTaster evaluates disease-causing potential of sequence alterations. Nat Methods 7: 575-6. doi: 10.1038/nmeth0810-575
31. Sethuraman G, Srinivas CR, D'Souza M, Thappa DM, Smiles L (2002) Dyschromatosis universalis hereditaria. Clin Exp Dermatol 27: 477-9. doi: 10.1046/j.1365-2230.2002.01129.x
32. Shellman YG, Lambert KA, Brauweiler A, Fain P, Spritz RA, Martini M, Janssen KP, Box NF, Terzian T, Rewers M, Horvath A, Stratakis CA, Robinson WA, Robinson SE, Norris DA, Artinger KB, Pacheco TR (2015) SASH1 Is Involved in an Autosomal Dominant Lentiginous Phenotype. J Invest Dermatol 135: 3192-4.
33. Stuhrmann M, Hennies HC, Bukhari IA, Brakensiek K, Nurnberg G, Becker C, Huebener J, Miranda MC, Frye-Boukhriss H, Knothe S, Schmidtke J, El-Harith EH (2008) Dyschromatosis universalis hereditaria:

evidence for autosomal recessive inheritance and identification of a new locus on chromosome 12q21-q23. Clin Genet 73: 566-72. doi: 10.1111/j.1399-0004.2008.01000.x

34. Stuhrmann M HH, Bukhari IA et al. (2008) Dyschromatosis uni versalis hereditaria: evidence for autosomal recessive inheritance and identification of a new locus on chromosome 12q21-q23. Clin Genet 73: 566–572.
35. Urabe K, Hori Y (1997) Dyschromatosis. Semin Cutan Med Surg 16: 81-5. doi: 10.1016/s1085-5629(97)80039-9
36. Wang K, Li M, Hakonarson H (2010) ANNOVAR: functional annotation of genetic variants from high-throughput sequencing data. Nucleic Acids Res 38: e164. doi: 10.1093/nar/gkq603
37. Webster GF, Berson D, Stein LF, Fivenson DP, Tanghetti EA, Ling M (2001) Efficacy and tolerability of once-daily tazarotene 0.1% gel versus once-daily tretinoin 0.025% gel in the treatment of facial acne vulgaris: a randomized trial. Cutis 67: 4-9.
38. Wen-Shyan Huang Y-WW, Kun-Che Hung,Pai-Shan Hsieh,Keng-Yen Fu, Lien-Guo Dai, Nien-Hsien Liou, Kuo-Hsing Ma,Jiang-Chuan Liu and Niann-Tzyy Dai (2018) High correlation between skin color based on CIELAB color space, epidermal melanocyte ratio, and melanocyte melanin content. PeerJ 6: e4815.
39. Xing QH WM, Chen XD, Feng GY, Ji HY, Yang JD, Gao JJ, Qin W, Qian XQ, Wu SN, He L. (2003) A gene locus responsible for dyschromatosis symmetrica hereditaria (DSH) maps to chromosome 6q24.2-q25.2. Am J Hum Genet 73: 377-82. doi: 10.1086/377007
40. Yongfei Yang G-BJ, Xuanjun Yang , Qiaoxiu Wang , Shanshan He , Shun Li , Christine Quach , Shihui Zhao , Fan Li , Zengqiang Yuan , Hye-Ra Lee , Hanbing Zhong , Chengyu Liang (2018) Central role of autophagic UVRAG in melanogenesis and the suntan response. Proc Natl Acad Sci U S A 115: E7728-E7737.
41. Yuta Araki KO, Toru Saito , Kazuhiko Matsumoto , Ken Natsuga , Junko Nishimoto, Yoko Funasaka , Yaei Togawa , Tamio Suzuki (2020) Five novel mutations in SASH1 contribute to lentiginous phenotypes in Japanese families. Pigment Cell Melanoma Res. doi: doi: 10.1111/
42. Zengyang Yu YG, Lian Cui , Yifan Hu , Qianqian Zhou , Zeyu Chen , Yingyuan Yu , Youdong Chen , Peng Xu, Xilin Zhang, Chunyuan Guo , Yuling Shi (2020) High-throughput transcriptome and pathogenesis analysis of clinical psoriasis. Journal of Dermatology Science 98: 109-118.
43. Zexi Xu YL, Dahong Wang, Daoqiu Wu, Jinyun Wang, Lian Chen ,Yinqian Deng, Jing Zhang, Zhixiong Wu, Xin Wan, Qianfan Liu, Hai Huan,g Pingsheng Hu, Jiawei Zeng, Ding'an Zhou (2020) Mutated SASH1 promotes Mitf expression in a heterozygous mutated SASH1 knockin mouse model. Int J Mol Med. 46: 1118–1134.
44. Zhang C, Li D, Zhang J, Chen X, Huang M, Archacki S, Tian Y, Ren W, Mei A, Zhang Q, Fang M, Su Z, Yin Y, Liu D, Chen Y, Cui X, Li C, Yang H, Wang Q, Wang J, Liu M, Deng Y (2013) Mutations in ABCB6 cause dyschromatosis universalis hereditaria. J Invest Dermatol 133: 2221-8. doi: 10.1038/jid.2013.145

45. Zhong WL, Wang HJ, Lin ZM, Yang Y (2018) Novel mutations in SASH1 associated with dyschromatosis universalis hereditaria. Indian J Dermatol Venereol Leprol. doi: 10.4103/ijdvl.IJDVL_360_17
46. Zhou D, Kuang Z, Zeng X, Wang K, Ma J, Luo H, Chen M, Li Y, Zeng J, Li S, Luan F, He Y, Dai H, Liu B, Li H, He L, Xing Q (2017) p53 regulates ERK1/2/CREB cascade via a novel SASH1/MAP2K2 crosstalk to induce hyperpigmentation. J Cell Mol Med 21: 2465-2480. doi: 10.1111/jcmm.13168
47. Zhou D, Wei Z, Deng S, Wang T, Zai M, Wang H, Guo L, Zhang J, Zhong H, He L, Xing Q (2013) SASH1 regulates melanocyte transepithelial migration through a novel Galphas-SASH1-IQGAP1-E-Cadherin dependent pathway. Cell Signal 25: 1526-38. doi: 10.1016/j.cellsig.2012.12.025

Figures

Figure 1

Pedigree and clinical features.

(**A**) Pedigree of members of a Chinese family with inherited dyschromatosis. * indicated that affected individuals whose skin tissues were taken for IHC analyses. (**B**) Representative image of irregularly shaped, asymptomatic hyper- and hypopigmented macules presenting on extremities and hips of the

proband (III-6) were showed in a generalized distribution manner. (**C, D and E**) Sporadic or disseminated hyper- and hypopigmented macules distributed on the neck and trunk of the II-3 affected individual, shanks of the II-10 one and facial regions of the II-11one. The Close-up views of II-3 and II-10 affected individuals could distinctly showed the hyper- and hypopigmented macules. Red arrows indicated the hyperpigmented macules, blue arrows indicated the hypopigmented macules.

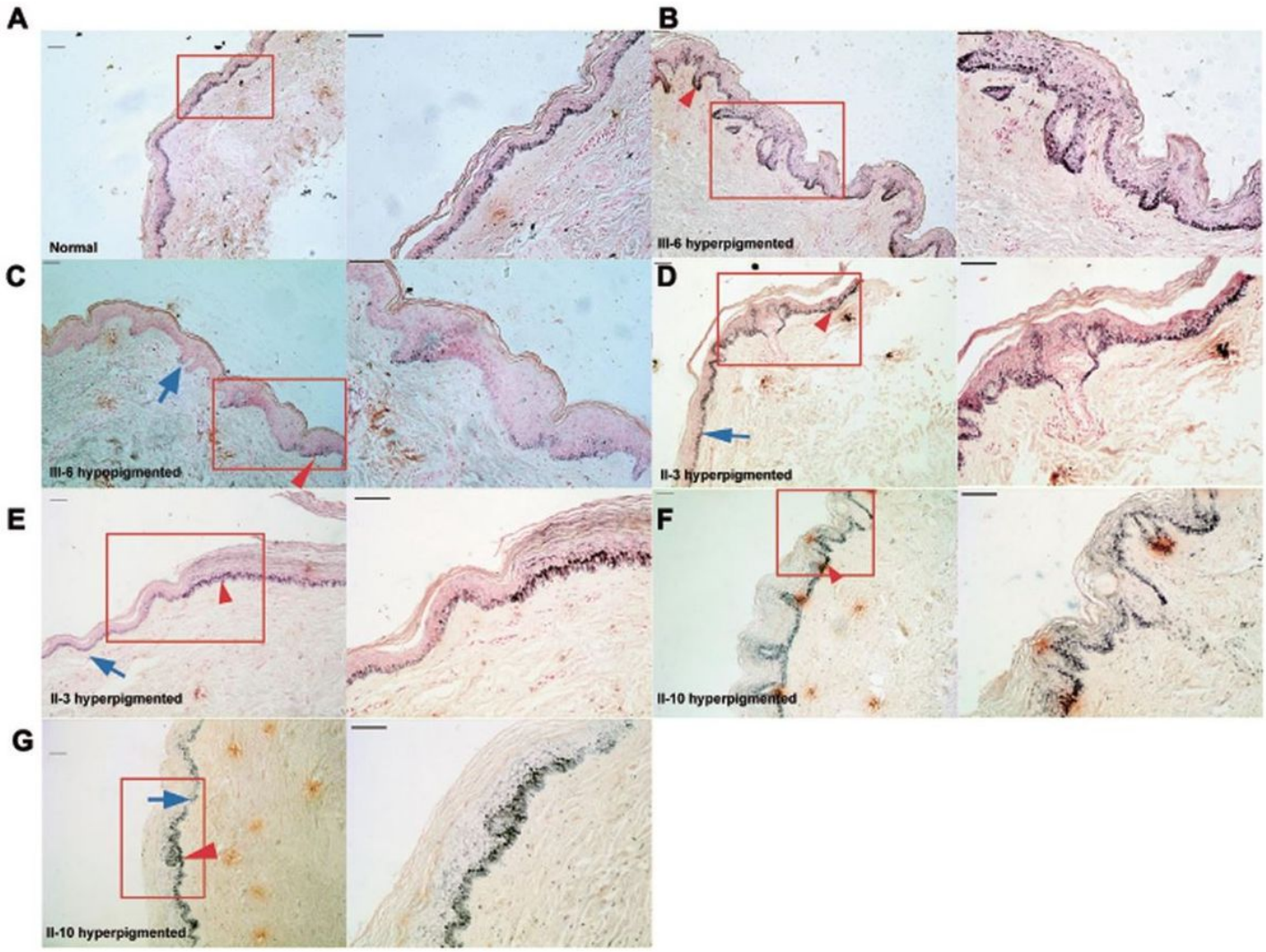

Figure 2

Heterogeneous distribution of melanin and increased melanin pigmentation were observed in the affected individuals' epithelial tissues in the family.

(**A**) Homogeneous melanin-stained positive epithelial cells of the normal control from a foreskin tissues from an early adolescence boy were located in the basal layers. (**B** and **C**) Heterozygous melanin distribution or mosaic like melanin distribution was observed in the affected epithelial layers in the hyperpigmented macules and the hypopigmented ones of the proband. Excessive melanin distribution was observed in both basal and superbasal layers. (**D**-**G**) Like those of the proband, mosaic like melanin

distribution and more melanin synthesis were observed in the affected epithelial layers in the hyperpigmented macules of the II-3 and the II-10 affected individual.

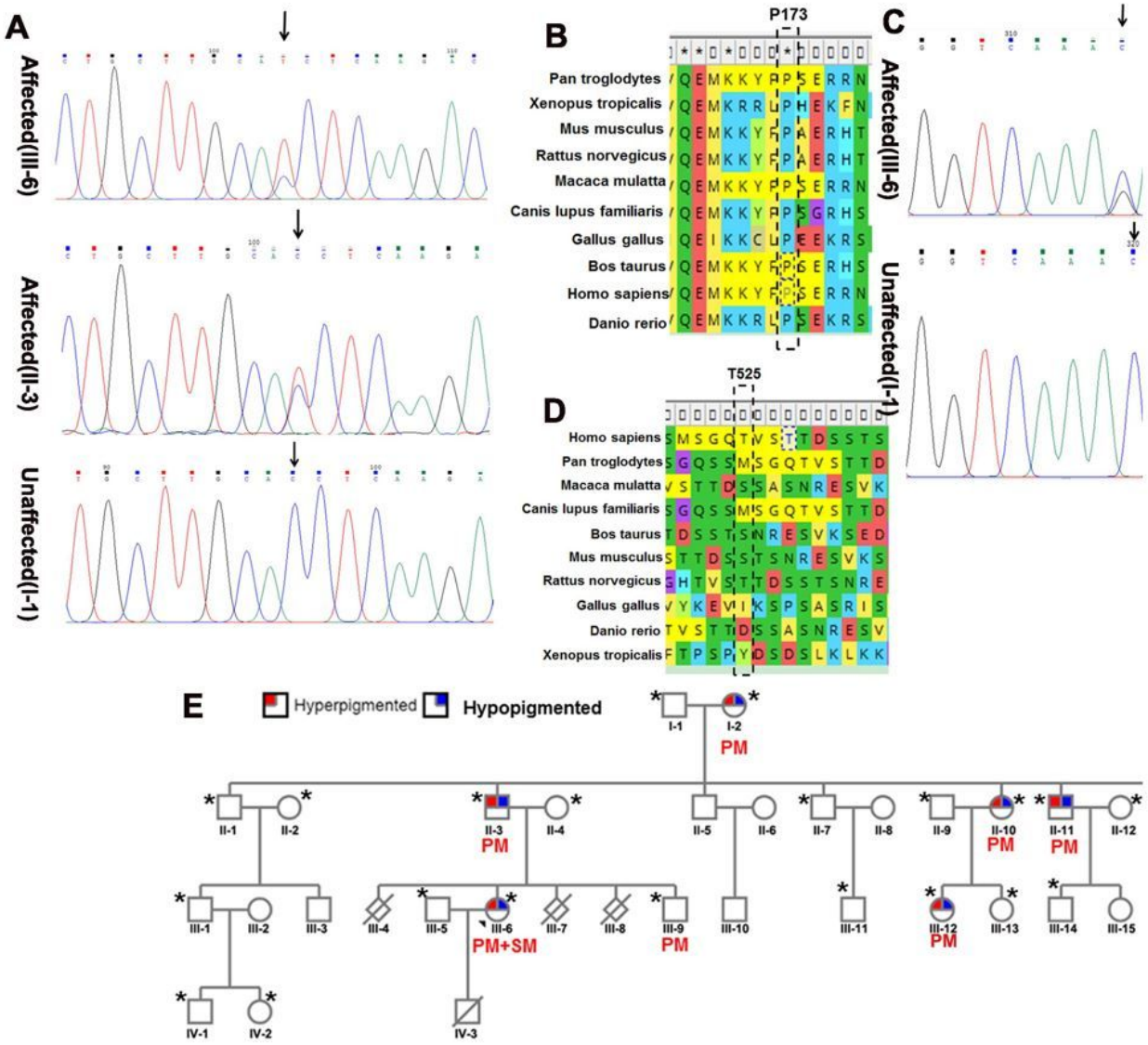

Figure 3

Identification of *PER3*^{P173S} SNP and *SASH1*^{T525R} mutation in the DUH family.

(**A**) Sequence chromatograms of an unaffected individual(I-1), an affected individual (II-3) and the proband (III-6) with a SNP in the *PER3* gene (c. C517T, p.P173S) in the family. Arrows indicate the location of the *PER3* SNP site identified in the proband, the affected individual and the unaffected individual. (**B**) The SNP site in *PER3* occurred in the evolutionarily conserved regions, which was framed by dotted line. (**C**) Sequence chromatograms of an unaffected individual (I-1) and the proband (III-6), with a heterozygous point mutation in the *SASH1* gene (c. C1574G, p.T525R) in the family. Arrows indicate the location of the *SASH1* mutation site identified in the proband and the unaffected individual. (**D**)The mutation site in *SASH1* occurred in the evolutionarily conserved regions, which was framed by dotted line.

A partial sequence of *SASH1* was compared with other species orthologs.(**E**) The family diagram to illustrate the affected individuals with the *PER3*^{P173S} SNP or/and *SASH1*^{T525R} mutation. Among 24 individuals whose blood was drew for DNA sequencing analyses, the *PER3*^{P173S} SNP was found in six affected individuals (I-2, II-3, II-10, II-11, III-6 and III-9) not in other unaffected individuals. Both *PER3*^{P173S} SNP and *SASH1*^{T525R} mutation were found in the proband (III-6). *indicated that the individuals whose blood was drew for exome sequencing and/or sanger sequencing. PM: *PER3* mutation, SM: *SASH1* mutation.

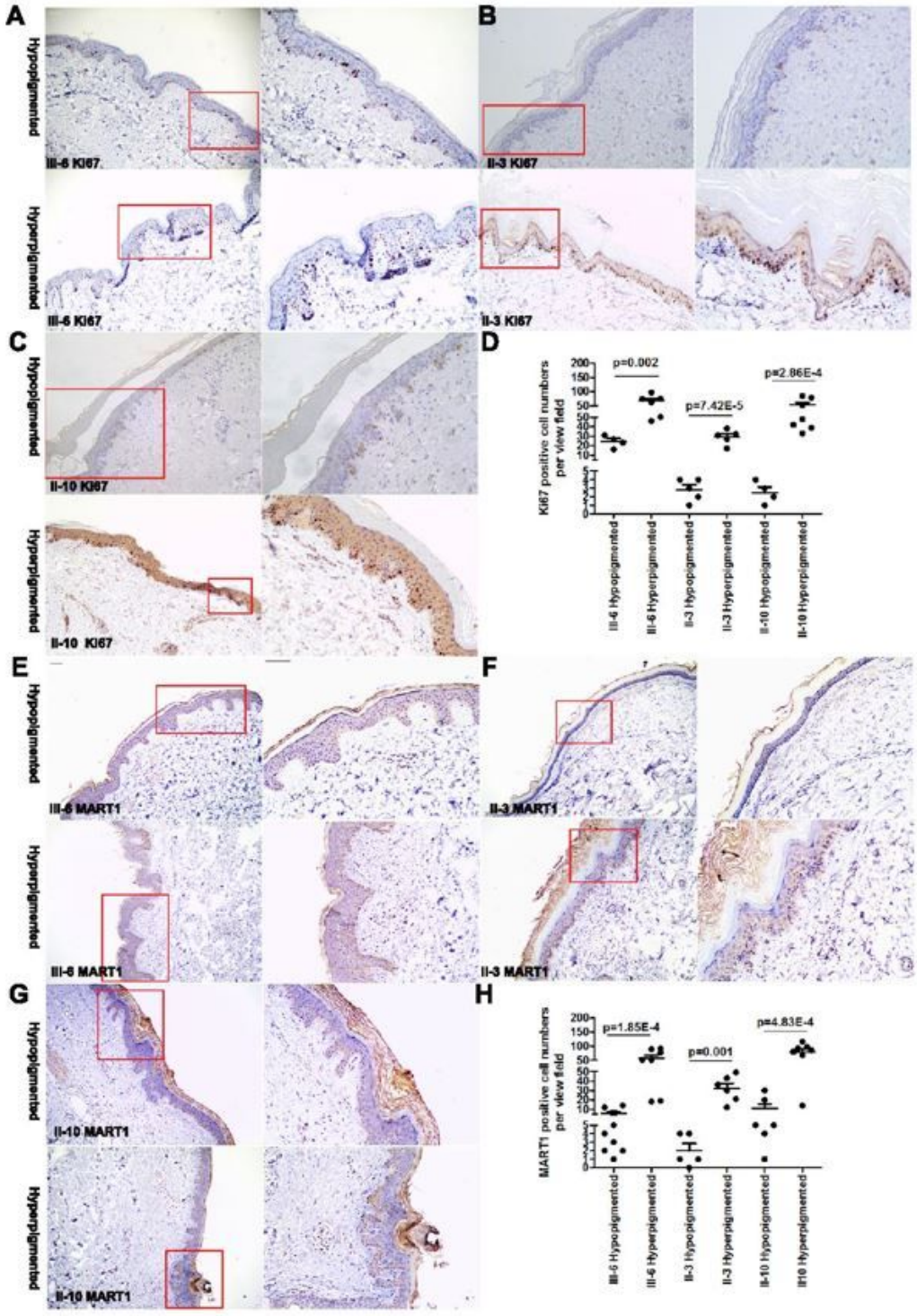

Figure 4

Increased numbers of melanocytes and epidermal cell proliferation in affected skin may be induced by *PER3*^{P173S} SNP and/or *SASH1*^{T525R} variant.

(**A**) About 2 fold more proliferating cells(Ki67 positive cells) in the affected epithelial tissues in the hyperpigmented macules of the proband(III-6) with SASH1 mutation and PER3 SNP(the bottom panels)

were induced compared with those in the hypopigmented macules of the proband (the upper panels). Representative figures of affected tissues which were highlighted by red boxes in the middle panels are amplified and showed in the right panels. Scale bar: 10 μm. (**B**) About 10 fold more proliferating cells in the affected epithelial tissues in the hyperpigmented macules of the II-3 affected individual with PER3 SNP(the bottom panels) were induced compared with those in the hypopigmented macules of the II-3 affected individual (the upper panels). (**C**) About 25 fold more proliferating cells in the affected epithelial tissues in the hyperpigmented macules of the II-10 affected individual with PER3 SNP(the bottom panels) were found compared to those in the hypopigmented macules of the II-10 affected individual (the upper panels). (**D**) The Ki67-positive cells in the affected epithelial tissues of hypopigmented macules and hyperpigmented ones in three affected individuals were counted respectively, and the numbers of Ki67-positive cells were statistically analyzed using one-way ANOVA. (**E**) About 5 fold more melanocytes (MART1-positive cells) in the affected epidermis in the hyperpigmented macules of the proband(III-6) with (the bottom panels) were induced compared to those in the hypopigmented macules of the proband (the upper panels). (**F**) About 15 fold more melanocytes in the affected epidermis in the hyperpigmented macules of the II-3 affected individual (the bottom panels) were induced compared to those in the hypopigmented macules of the II-3 affected individual (the upper panels). (**G**) About 10 fold proliferating cells in the affected epidermis in the hyperpigmented macules of the II-10 affected individual (the bottom panels) were found compared with those in the hypopigmented macules of the II-10 affected individual (the upper panels). (**H**) The MART1-positive cells in the affected epidermis of hypopigmented macules and hyperpigmented ones in three affected individuals were counted respectively, and the numbers of MART1-positive cells were statistically analyzed using one-way ANOVA.

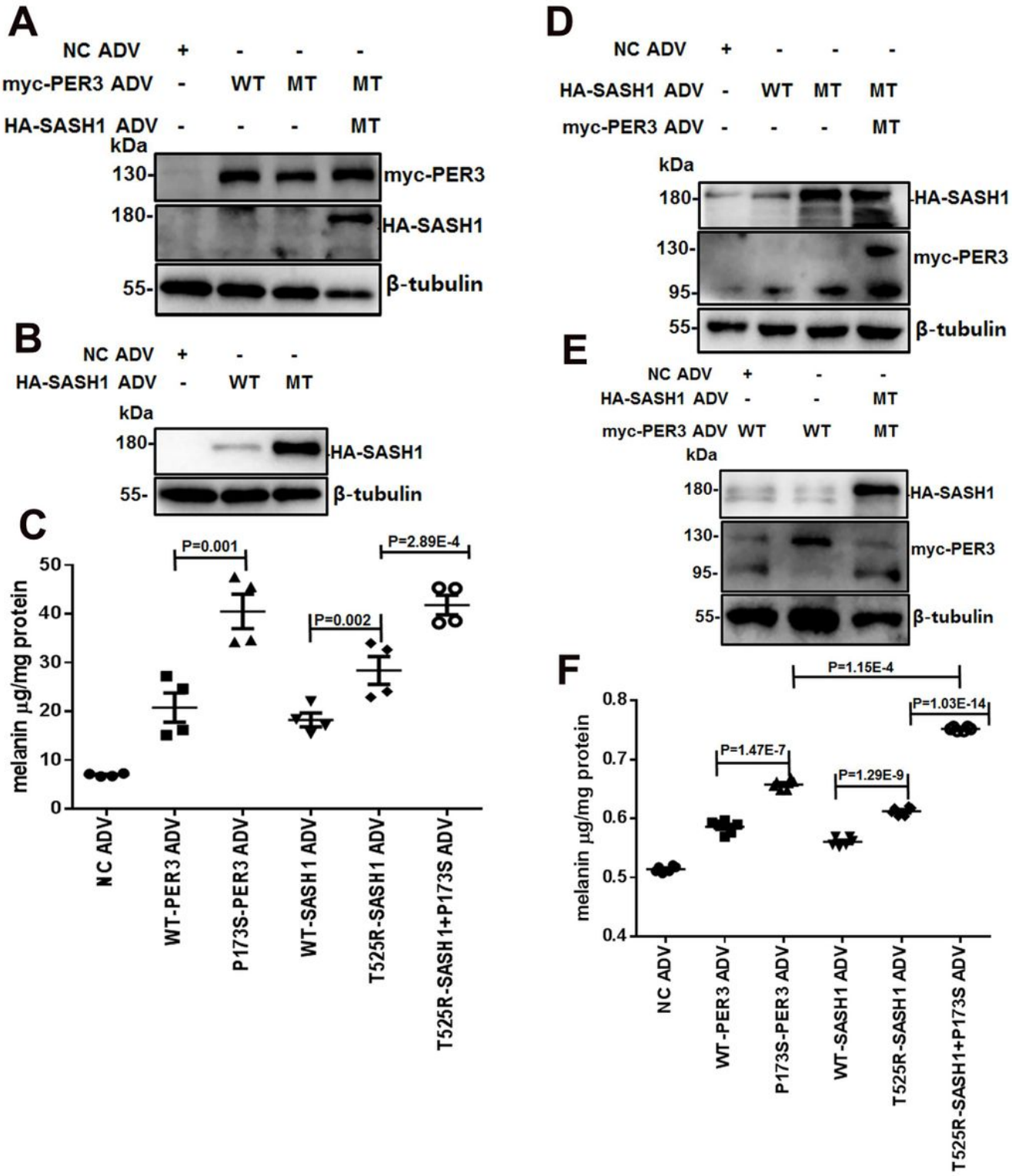

Figure 5

Increased melanogenesis in melanoma cells was induced by *PER3*^{P173S} SNP or *SASH1*^{T525R} variant, and augmented by the combination of *PER3*^{P173S} SNP and *SASH1*^{T525R} variant.

(**A-B**) T525R-SASH1 was upregulated in B16 cells. The expression of wild type or mutated PER3, and wild type SASH1 and mutated SASH1 in B16 affected cells with combined adenovirus was identified by

western blot. B16 cells were infected with the adeasy014- pAdEasy-EF1-MCS-CMV-EGFP adenovirus containing wild type *PER3* , mutant type *PER3* P173S, wild type *SASH1* and *SASH1* T525R mutant as per different combinations. At 60hr after infection，cells were lysed and subjected to western blot. (**C**) Increased melanin content in B16 cells was induced by *PER3*^{P173S} SNP or *SASH1* ^{T525R} mutant, and augmented by the combination of *PER3*^{P173S} SNP and *SASH1* ^{T525R} mutant. B16 cells were infected with the adeasy014- pAdEasy- EF1- MCS-CMV-EGFP adenovirus expressing *PER3* and *SASH1* as per different combinations. At 60hr after infection，cells were lysed and the melanin content was quantified according to the manufacture protocol. (**D-E**) T525R-SASH1 was upregulated in SK-MEL-1 cells. The expression of wild type or mutated PER3， and wild type *SASH1* and mutated *SASH1* in SK-MEL-1 affected cells was identified by western blot. (**F**) Enhanced melanin content in SK-MEL-1 cells was induced by *PER3*^{P173S} SNP or *SASH1* ^{T525R} mutant, and augmented by the combination of *PER3*^{P173S} SNP and *SASH1* ^{T525R} mutant.

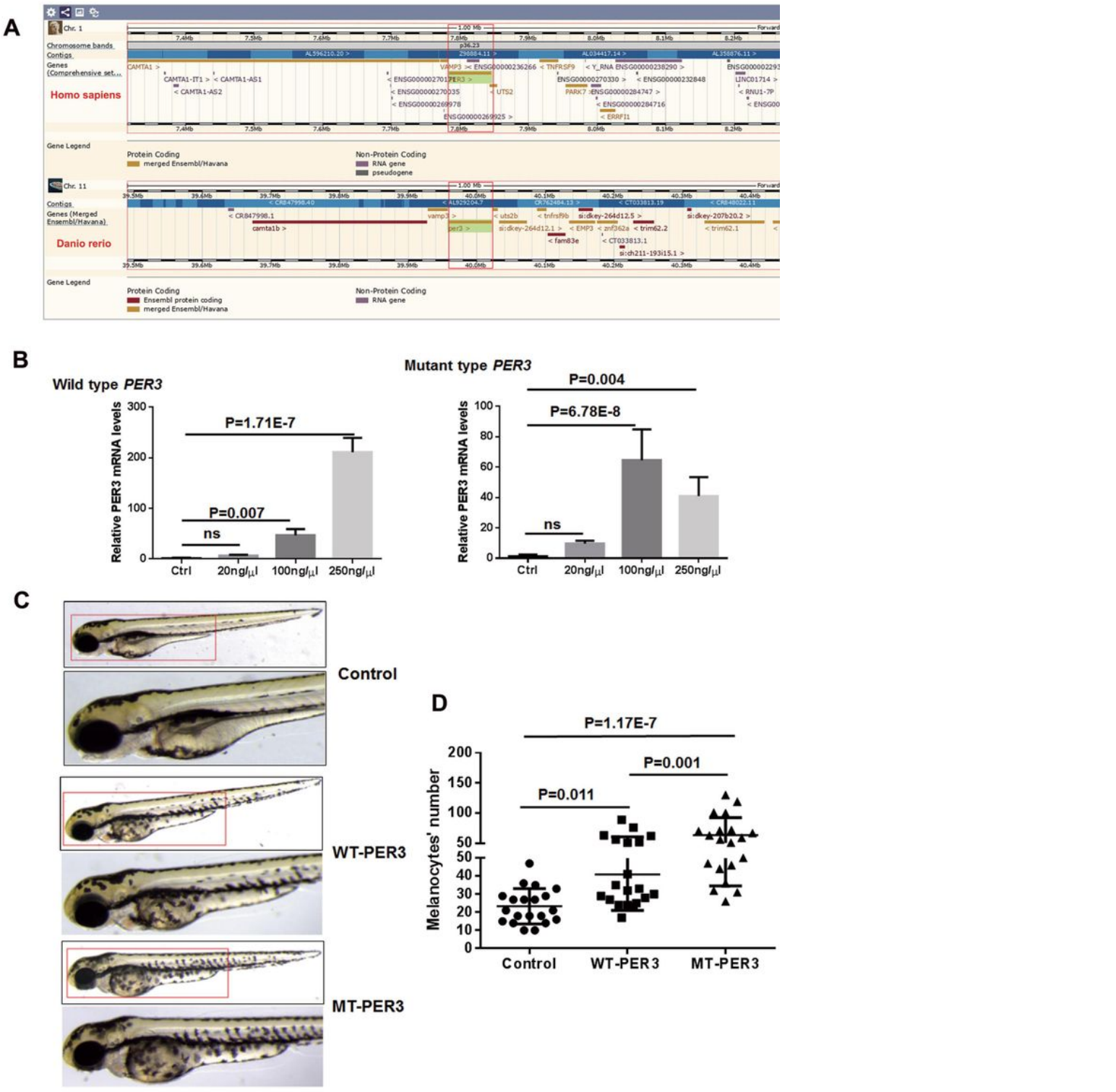

Figure 6

PER3^{P173S} SNP i**s required for melanocyte proliferation in zebrafish *in vivo*.**

(**A**) Human *PER3* and zebrafish *per3 are* orthologous genes. Homology of gene sequence of *PER3* analyses from Ensembl database indicated human *PER3* and zebrafish *per3* were homologous gene, and there are collinear genes vamp3 (vamp3), UTS2 (uts2b), etc. (**B**) Quantitative RT-PCR detected that wild

type and mutant type *PER3* were expressed in zebrafish at 24hpf. (**C**) Representative images of 72hpf zebrafish embryos injected with the transcript of wild type *PER3* and $PER3^{P173S}$ SNP or Control. (**D**) Quantitative measurement shows highly proliferative melanocytes were induced by $PER3^{P173S}$ SNP compared with those of the control group and wild type *PER3*.

Supplementary Files

This is a list of supplementary files associated with this preprint. Click to download.

- 202205HGFigureS1.eps
- 202205HGFigureS2.eps
- 202205HGFigureS3.eps
- 202205FigureS4.eps
- 202205FigureS5.eps
- 202205FigureS6.eps
- 20220518TableS1Theprimerssequences.docx
- 20220518TableS2clinicalphenotypes.docx
- 20220518TableS3AffectedPER3SNV.docx
- 20220518TableS4UnaffectedPER3SNP.docx
- 20220518TableS5Varsomepathogenicity.docx
- 20220518TableS6AffectedSFTA3SNV.docx
- 20220518TableS7KYNUSNV.docx
- 20220518TableS8ABCB6SNV.docx
- 20220518TableS9SASH1SNV.docx
- 20220518TableS10GLMNSNV.docx
- 20220518TableS11theremaining24gene.docx